Nanoscale

Accepted Manuscript

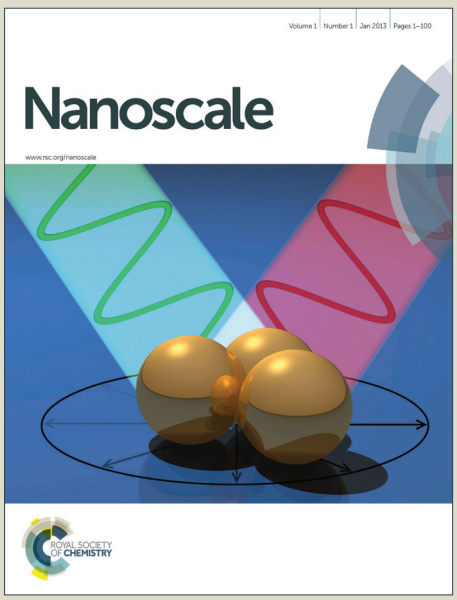

ROYAL SOCIETY OF CHEMISTRY

www.rsc.org/nanoscale

ARTICLE TYPE www. rsc.org/xxxxxx | XXXXXXXX

Near-infrared Absorbing Polymer Nano-particle as a Sensitive Contrast Agent for Photo-acoustic Imaging†

Hiroyuki Aoki,*[a,b] Mayumi Nojiri,[a] Rieko Mukai,[b] and Shinzaburo Ito[a]

Received Xth XXXXXXXXXX 20XX, Accepted Xth XXXXXXXXX 20XX
First published on the web Xth XXXXXXXXXX 200X
DOI: 10.1039/b000000x

Polymer nano-particles (PNP) with a near-infrared (NIR) light absorption were prepared by the nano-emulsion method to develop contrast agents for photo-acoustic (PA) imaging. The PNP containing silicon naphthalocyanine showed a high absorption coefficient up to 10^{10} M^{-1} cm^{-1}. This is comparable to plasmonic gold nano-particles, which have been studied as PA contrast agents. For the PNP larger than 100 nm, the enhancement of the PA signal was observed compared to the gold nano-particle with the similar absorption coefficient and size. In the case of the PNP, the heat by the light absorption is confined in the particle due to the low thermal diffusivity of polymer materials. We showed that the strong thermal confinement effect of PNP results in the enhancement of the efficiency of the PA signal generation and that the PA intensity can be enhanced by the increase of the Grüneisen parameter of the matrix polymer of PNP. The PA signal from the PNP of poly(methyl methacrylate) was 9-fold larger than that from gold nano-particles with the same absorption coefficient. We demonstrated that in the *in vivo* PA imaging the detection limit of PNP was on the order of 10^{-13} M. The NIR absorbing PNP will be a promising candidate of a sensitive contrast agent for PA imaging.

Introduction

Photo-acoustic (PA) imaging has attracted much attention as a modality with both advantages of optical and acoustic imaging techniques[1–3]. The PA imaging technique provides three-dimensional information on the spatial distribution of light absorbing objects at the deep inside of a living body. *In vivo* applications of the PA imaging with contrast agents have been extensively studied for the visualization of tumors and sentinel lymph nodes[4–8]. Exogenous contrast agents are required to generate the large PA signal to overcome the high background signal from strong light absorbers in tissues such as hemoglobin and melanin. Organic dyes, carbon nanotubes, and nano-structured metal particles have been studied as the contrast agents for the PA imaging.[4–16] Among such the contrast agents, gold nano-particles are promising materials to generate the large PA signal. In order to increase the PA signal, the absorption coefficient at a near-infrared (NIR) range of 700 – 900 nm should be maximized because the PA intensity is proportional to the absorbed energy of a laser pulse. The gold nano-particles strongly absorbs the light by the localized plasmon resonance and the absorption wavelength can be controlled by the morphology of the particle. Gold nano-rods and nano-cages with sizes from tens to hundreds nm have been studied as sensitive contrast agent in the NIR region.[7–13] Since the sound pressure of the PA wave is affected by not only the increase of the absorption coefficient but also the heat transfer from the nano-particle to the surrounding dispersion medium, the thermal resistance at the particle surface affects the intensity of the PA signal.[11] In the application of nano-particles in *in vivo* imaging, the blood circulation and target specificity is dependent on the particle size and the surface properties.[17,18] Because the absorption coefficient and spectrum of gold nano-particles is determined by the size and structure of the particle, the modification of the structure and surface to optimize the localization and disposition in an *in vivo* condition should affect the optical properties of gold nano-particles. Therefore, the optical properties and the particle structure should be independently controlled to design the contrast agent for the PA imaging. In this study, we introduce nano-particles of polymer materials as the highly sensitive contrast agent for the PA imaging. The polymer nano-particle (PNP) have been extensively studied as molecular probes to visualize tumor sites[19–21]. The particle size and surface properties governing the blood circulation and target specificity can be controlled independently of the optical properties. We revealed the key factors to enhance the PA signal from nano-particles and showed that the PNP containing an organic dye showed the 30-fold greater PA signal in the NIR region than gold nano-particles. We also

† Electronic Supplementary Information (ESI) available: [details of any supplementary information available should be included here]. See DOI: 10.1039/b000000x/

[a]*Department of Polymer Chemistry and* [b]*Advanced Biomedical Engineering Research Unit, Kyoto University, Nishikyo, Kyoto 610-8510, Japan. Fax: +81-75-383-2617; Tel: +81-75-383-2613; E-mail: aoki@photo.polym.kyoto-u.ac.jp*

performed the *in vivo* PA imaging of a mouse to demonstrate the high sensitivity of the PNP contrast agent.

Experimental section

Nano-particles of a polymer containing a dye were prepared by a nano-emulsion method.[22,23] Polymers used here are polystyrene (PS), poly(methyl methacrylate) (PMMA), poly(ethyl methacrylate) (PEMA), poly(*n*-butyl methacrylate) (PnBMA), poly(*iso*-butyl methacrylate) (PiBMA). Silicon 2,3-naphthalocyanine bis(trihexylsilyloxide) (SiNc, Aldrich), 1,1'-dioctadecyl-3,3,3',3'-tetramethylindodicarbocyanine, 4-chlorobenzenesulfonate salt (DiD, PromoCell), and 1,1'-dioctadecyl-3,3,3',3'-tetramethyl indotricarbocyanine iodide (DiR, PromoCell) were used as dyes. A typical procedure of the preparation of PNP is as follows. A chloroform solution of a polymer and a dye was added to 10 mL of an aqueous solution of a surfactant: sodium dodecyl sulfate (SDS, Tokyo Chemical Industry) or polyoxyethylene sorbitan monolaurate (Tween 20, Tokyo Chemical Industry). The emulsion of the polymer solution was prepared by the ultra-sonication at a frequency of 22.5 kHz and a power of 20 W (Microson XL2000, Misonix) for 30 s at 0°C. The PNP was obtained after the removal of chloroform by stirring the sample solution at 40°C for 90 min. The diameter of the nano-particle was measured by the dynamic light scattering method (ELSZ-2, Otsuka Electronics) and transmission electron microscopy (JEM-2100F, JEOL). A water dispersion of gold nano-rods (80×25 nm) was purchased from Nanopartz.

The PA intensity measurement was carried out by a home-built apparatus. The sample solution in a polystyrene cell with an optical path length of 1 mm was immersed in a temperature-controlled water bath ($\pm$ 0.1°C). The samples were illuminated by laser pulses with a width of 800 ps and an energy of 40 μJ from a dye laser pumped by a nitrogen laser (OB-401 and OB-4300, Optical Building Blocks, respectively). The acoustic signal was detected by a hydrophone (H9C, Toray Engineering) with a band width of 0.5 – 10 MHz through an amplifier (Model 5682, Olympus NDT). A schematic illustration of the apparatus is shown in Figure S1a in Supplementary Information. All of the measurements were carried out at the concentration with an absorbance of 0.5 at a peak wavelength. For *in vivo* imaging, normal nude mice (7 weeks old, male; BALB/c slc-nu/nu, Japan SLC) were used. Fluorescence imaging of mice was carried out by an IVIS Lumina system (Xenogen). The PA imaging was performed by a home-built system. A mouse was irradiated by pulses at an energy density of 20 mJ cm^{-2} from a Ti:Sapphire laser (LT-2211A, LOTIS TII). The PA signal from the irradiated point was detected by a focused transducer (V383, Olympus NDT) with scanning the mouse on a motorized XY stage (SGAM20-35XY, Sigma Koki) equipped with a temperature controller to obtain a PA image (Figure S1b). The mice were subcutaneously injected with the PNP and gold nano-rod dispersed in phosphate-buffer saline (PBS). During the imaging, the mice were kept on the stage under an anesthetized condition with isoflurane gas. All animal experiments were performed according to the Institutional Guidance of Kyoto University on Animal Experimentation and under permission by animal experiment committee on Faculty of Engineering, Kyoto University.

Results and discussion

The nano-emulsion method allowed the preparation of the PNP from various hydrophobic polymers and dyes. For example, we prepared the PNP from polystyrene (PS) and poly(alkyl methacrylate)s with the phthalocyanine, carbocyanine, and porphyrin derivatives. A transmission electron microscopy image of PNPs consisting of PS and 2,3-naphthalocyanine bis(trihexylsilyloxide) (SiNc) is shown as the inset of Figure 1a, indicating the spheric particles with a diameter of 100 nm. The PNP with a diameter in the range of 40 – 200 nm was available by varying the concentration of polymers and surfactants (the results of the dynamic light scattering measurement are shown in Figure S2a in the Supporting Information). The PA signal from the dispersion of the 100-nm PNP is shown in Figure 1a. The waveform of the PA signal was dependent on the shape of the illuminated volume which is determined by the optical path length of the sample cell and the beam profile. On the other hand, the PA waveform was not dependent on the properties of PNP: the size, dyes, surfactants, and polymers as shown in Figures S2b and S3. We discuss the effect of the properties of PNP on the intensity of the PA signal, which is defined as the peak-to-peak amplitude normalized by the light energy absorbed by the solution. The absorption band of the PNP can be easily tuned in a wide range of wavelengths by the choice of dyes. Figure 1b shows the absorption spectra and the wavelength dependence of the PA intensity for the PNP containing SiNc, 1,1'-dioctadecyl-3,3,3',3'-tetramethylindodicarbocyanine 4-chlorobenzenesulfonate salt (DiD), and 1,1'-dioctadecyl-3,3,3',3'-tetramethyl indotricarbocyanine iodide (DiR). The PA spectra were in good agreement with the corresponding light absorption, indicating the tunability of the excitation wavelength of the PNP in the PA measurement. In the design of the PA imaging contrast agent, the molar absorption coefficient is one of the most important factors to obtain a high intensity at a low concentration because the PA intensity is proportional to the heat supplied by the light absorption. SiNc has a molar absorption coefficient of 5.7×10^5 $M^{-1}cm^{-1}$ with a sharp absorption band at 780 nm. Therefore, the PNP containing SiNc would be a most effective contrast agent for the PA imaging with a strong light absorption in the

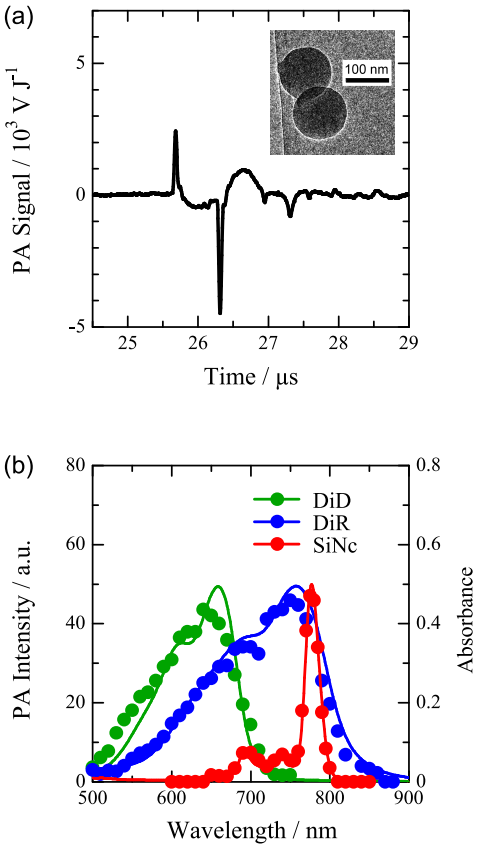

Fig. 1 Photo-acoustic wave and wavelength dependence of photo-acoustic intensity from PNP. (a) The waveform of the PA signal from the PNP of PS and SiNc with a diameter of 100 nm dispersed in an optical cell with a path length of 1 mm. The inset indicates a transmission electron microscopy image of the PNP. (b) The wavelength dependence of the photo-acoustic intensity for SiNc (red), DiD (green), and DiR (blue). The filled circles and solid curves indicate the photo-acoustic intensity and light absorption, respectively.

optical window region for biological tissues. The absorption coefficient of the dye-doped PNP can be increased by the increase of the ratio of the dye to PS in the PNP. However, the increase of the dye fraction resulted in the broadened size distribution. It was found that the maximum fraction of SiNc was 30 wt% to obtain the mono-disperse PNP. The highest molar absorption coefficient of the PNP with a diameter of 100 nm was 2.0×10^{10} $M^{-1}cm^{-1}$, which is on the same order as that of the gold nano-particle with a similar size.[24]

Figure 2 shows the particle size dependence on the PA intensity. This indicates that the PA intensity is not dependent on the particle size for the PNP less than 100 nm and that the signal intensity considerably increases with the increase of the size in the diameter range of $>$ 100 nm. The photo-acoustic

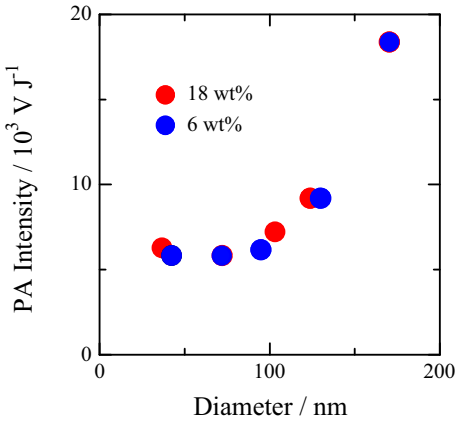

Fig. 2 Relationship between the PA signal and the particle size for the PNP containing SiNc with a dye fraction of 6 and 18 wt%. The PA measurements were carried out at an absorbance of 0.5 in an optical cell with a path length of 1 mm.

pressure, p, is given as

$$p = \Gamma \eta H, \quad (1)$$

where Γ, H, and η are the Grüneisen parameter, the energy supplied by a laser pulse, and the conversion efficiency from light into heat, respectively[1]. The Grüneisen parameter is the conversion efficiency from heat to sound pressure and defined as

$$\Gamma = \beta \kappa / \rho C_p, \quad (2)$$

where β, κ, ρ, and C_p are the volumetric thermal expansion coefficient, compressive modulus, density, and heat capacity at constant pressure of the expanding substance by the laser pulse irradiation, respectively. As described in the experimental section, the PA measurement was performed at an absorbance of 0.5. Therefore, the energy supplied by a laser pulse was the same (27 μJ/pulse) for all of the sample solutions. Therefore, this result indicates that the parameters η and/or Γ are dependent on the particle size. Now we consider the conversion efficiency from light to heat, η. Fluorescence emission is another relaxation process of the absorbed light energy for SiNc. Since the emission quantum yield of SiNc in the PNP is less than 0.01 as shown in Table S1 of Supplementary Information, most of the absorbed light energy is converted to heat. Therefore, it can be said that the heat supplied to the PNP by the laser pulse, ηH, is the same for the PNPs with diameters of 40 – 200 nm. Consequently, according to the above equation, the size dependence for the PNP larger than 100 nm seems to indicate that the Grüneisen parameter is dependent on the particle size.

The apparent size dependence of the Grüneisen parameter for the PNP dispersion can be explained by the heat transfer

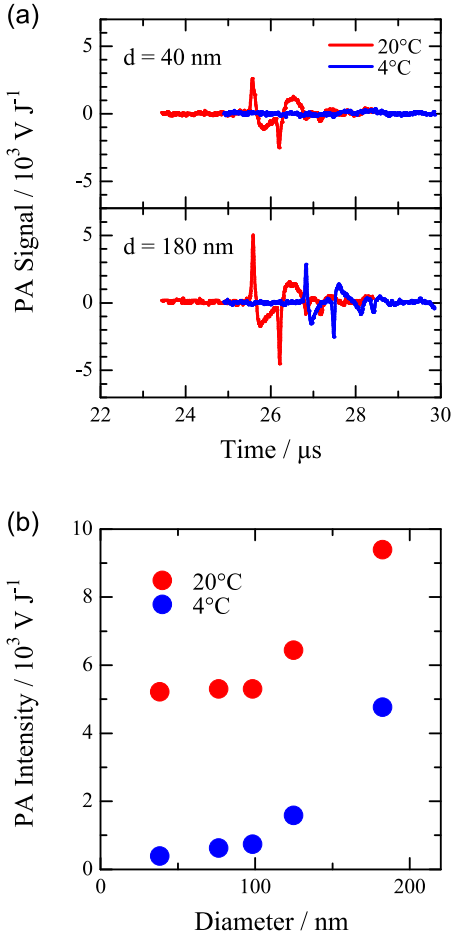

Fig. 3 Temperature dependence of the photo-acoustic signals. (a) The waveform at 4 and 20°C for the PNPs with diameters of 40 and 180 nm with the dye fraction of 5 wt%. (b) The relationship between the particle size and the signal intensity. The red and blue symbols indicate the data at 4 and 20°C.

from PNP to water. After the laser irradiation, some part of the heat by the light absorption of the particle diffuses into the water medium. Consequently, the sound pressure consists of the contributions from the volume expansion of water and PNP. The heat partitioning in the PNP and the water medium is dependent on the particle size; therefore, Γ was apparently dependent on the diameter of the PNP. In order to examine the sound pressure components of water and PNP, the photo-acoustic signals at 4 and 20°C were compared. Since the thermal expansion coefficient of water is zero at 4°C, the photo-acoustic signal from the water medium should be negligible.[25] The PA intensity at 4°C corresponds to the acoustic pressure component only by the volume expansion of the PNP. Thus, the comparison of the signals at 4 and 20°C clarifies the heat transfer from the PNP to water. The PA

Table 1 Comparison of PA intensity between PNP and Au-NR

	Size / nm	ε / $M^{-1}cm^{-1}$	A / 10^3 V J^{-1}
Au-NR-80†	80 × 25	1.1×10^{10}	1.59
Au-NR-200†	200 × 50	6.8×10^{10}	1.40
PNP-PS-94‡	94	1.2×10^{10}	4.74
PNP-PS-160‡	160	5.0×10^{10}	10.6

†Au-NRs were purchased from Nanopartz, Inc. ‡The dye fractions of PNP-PS-94 and PNP-PS-160 were 25 and 20 wt%, respectively.

signals at 4 and 20°C for the PNPs of PS with diameters of 40 and 100 nm are shown in Figure 3a. The PA signal for the 40-nm PNP markedly decreased at 4°C, indicating that most of the heat supplied by the laser pulse transferred to water and the volume expansion of water resulted in the PA wave. On the other hand, the PA signal was observed from the 100-nm PNP at 4°C. This indicates that the PA wave was generated by the volume expansion of the PNP. Figure 3b shows the size dependence of the PA signals at 4 and 20°C. For the PNP less than 100 nm, the PA signal was considerably small at 4°C compared to that at 20°C, indicating the fast heat transfer from the PNP to water. On the other hand, the PA signal increased with the increase of the diameter of the PNP larger than 100 nm. This indicates that the heat remaining in the PNP increased with the increase of the particle size. The sound pressure component of the PNP at 20°C is 50% for the PNP with a diameter of 180 nm, whereas that for the 40-nm PNP is as small as 6%.[26] The values of Γ for water and PS are 0.11 and 0.73 at 20°C, respectively. Therefore, the efficient generation of the PA signal is expected for the volume expansion of the PNP consisting of PS. The heat supplied to a PNP by a laser pulse is proportional to the cube of the particle size because the light absorption linearly depends on the amount of SiNc in a PNP. The heat transfer occurs across the surface of the PNP. On the other hand, the surface area of a PNP increases dependent on only the square of the particle size. Consequently, the larger the particle size, the larger part of the heat supplied by the laser pulse remains in the PNP. Thus, the enhancement of the PA signal of the larger PNP can be explained by the reduction of the heat transfer from the PNP to the water medium.

Gold nano-particles have been extensively studied as the contrast agent in the PA imaging. The PA intensity from the PNP was compared with that from the gold nano-rod (Au-NR), which has been used as a strong contrast agent for the PA imaging in the near infrared region[7,12,13]. Table 1 summarizes the molar absorption coefficient ε and the PA intensity A of the PNPs and the Au-NRs. The PA intensities from the 200 × 50-nm and 80 × 25-nm Au-NRs were almost the same. The

photo-acoustic signal of PNP is larger than that of Au-NR with the similar absorption coefficient and particle size. This indicates that the apparent conversion efficiency from light to sound for PNP is far larger than that for Au-NR, whereas the values of Γ for gold and PS are evaluated to be 2.9 and 0.73 from their physical constants, respectively. This is due to the difference in the thermal diffusivity of PS and gold (0.086 and 127 mm^2s^{-1}, respectively). The diffusion length of the heat in gold in 1 ns is estimated to be 350 nm. Therefore, the heat in an Au-NR less than a few hundred nm transfers to the surrounding water medium in the pulse duration. We observed that the photo-acoustic signal from the Au-NR almost vanished at 4°C (see Figure S4 in Supplementary Information), indicating the no contribution of the thermal expansion of the Au-NR on the acoustic wave generation. In the photo-acoustic wave generation process from gold nano-particles, the heat by the light absorption rapidly transfers to the surrounding water from the gold particle, resulting in the PA wave only by the volume expansion of water with Γ of 0.11. This also results in the weak size dependence of the PA signal from the Au-NRs shown in Table 1. On the other hand, the heat absorbed by a laser pulse remains in the PNP in the time scale of the sound generation as indicated by Figure 3. This resulted in the strong PA wave due to the expansion of both the water medium and the particle of PS with the large Grüneisen parameter. Thus, although the Grüneisen parameter of PS is smaller than that of gold, the PNP of PS shows much higher light-acoustic conversion efficiency compared to Au-NR. The PA intensity from the PNP can be enhanced by the reduction of the heat diffusion by the increase of the diameter. PNP-PS-160 showed the further enhancement of the PA signal due to the decreased thermal diffusion compared to PNP-PS-94. The PA intensities normalized by the particle concentration were 3.49 V $J^{-1}pM^{-1}$ for Au-NR and 106 V $J^{-1}pM^{-1}$ for PNP-PS-160, indicating the 30-fold enhancement of the PA signal for the PNP compared to the Au-NR. Moreover, the durability against the laser pulse was examined (Figure S5). The photo-acoustic intensity of Au-NR decreased to 75% from the initial value after 400 pulses. This is due to the decrease of the absorption coefficient of Au-NR by the structural change to a spherical shape[27]. On the other hand, the PNP showed no bleaching of the photo-acoustic intensity even after more than 3000 laser shots. Thus, the PNP shows the large photo-acoustic conversion efficiency and the high durability against the repeated pulse irradiation.

The PA intensities of the PNPs consisting of different polymers were compared. The PNPs of the following polymers with SiNc were prepared: PMMA, PEMA, PnBMA, PiBMA, and PS, which has the Grüneisen parameter of 1.38, 1.17, 0.87, 0.85, and 0.71, respectively[28–30]. Figure 4 shows the relationship between the PA intensity and the Grüneisen parameter of the polymers of the PNPs. The red circles in this figure indicate the PA intensity for the PNPs with the diameter of 123 ± 1 nm and the molecular absorption coefficient of (2.4 ± 0.2) × 10^{10} $M^{-1}cm^{-1}$. This indicates that the PA intensity increased with the increase of the Grüneisen parameter of the matrix polymer of the PNP. On the other hand, the black data points in Figure 4 show the polymer dependence of the PA intensity for the PNPs with the diameter of 46 ± 5 nm, indicating that the PA intensity is not dependent on the Grüneisen parameter. As mentioned above, because the heat supplied to the small particle rapidly transfers to the surrounding water, the PA wave was generated by the volume expansion of water. Therefore, the PA intensity is not dependent on the physical properties of the matrix polymer. For the PNP larger than 100 nm, the heat transfer is relatively slow. The acoustic pressure consists of the contribution of the thermal expansion of the water medium and the PNP. Since the thermal diffusivity of the polymer materials shows similar values of ca. 0.1 mm^2s^{-1}, the pressure component from the water medium can be assumed to be the same for the PNPs of these polymers. Therefore, the increase of the PA intensity from the PNP of PMMA is attributed to the increase of the pressure component due to the thermal expansion of the nano-particle dependent on the Grüneisen parameter. This result indicates that the thermal confinement in the nano-particle and the large Grüneisen parameter of the material of PNP is the most important factors to design the nano-particle contrast agent for the PA imaging. The heat transfer is a key factor for the gold nano-particle contrast agent for the PA imaging; however, the strategy for the design of the high sensitivity agent is completely different. Because gold inherently has a high thermal diffusivity, the heat transfer

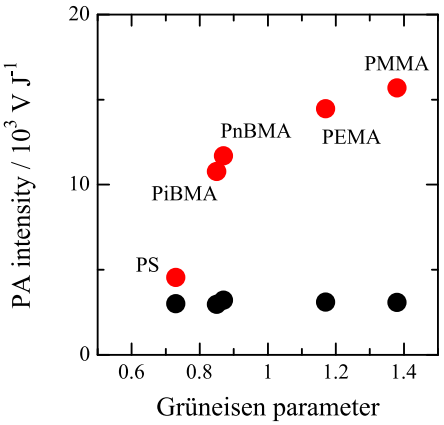

Fig. 4 Photo-acoustic intensity dependent on polymer materials. The PA intensity is plotted against the Grüneisen parameter for the polymer materials: PMMA, PEMA, PnBMA, PiBMA, and PS. The red and black circles indicate the PA intensity for the PNPs with the diameters of 123 and 46 nm, respectively.

from a nano-particle of gold to the water medium cannot be suppressed. The volume expansion of water is the origin of the PA wave from the dispersion of the gold nano-particles. Therefore, the rapid volume expansion by the increase of the heat transfer rate results in the enhancement of the photo-acoustic pressure[11,31,32]. On the other hand, the thermal diffusion in polymeric materials is slow compared to that of metal; therefore, the heat can be confined in the particle, resulting in the strong PA wave by the volume expansion of the PNP with a large Grüneisen parameter. Therefore, the sensitivity can be increased by the suppression of the heat transfer to the surrounding medium and the use of polymeric materials with a large Grüneisen parameter. Considering such the enhancement mechanism, the PNP of PMMA emitted the 9-fold larger PA signal compared to that from Au-NR.

Hemoglobin in red blood cells (RBCs) is an endogenous strong light absorber, resulting in the strong PA signal from blood vessels. In order to use the PNP as a contrast agent in the *in vivo* PA imaging, it is necessary to generate the comparable or greater PA signal than that from blood. The PA intensity from PNP with a diameter of 160 nm and an absorption coefficient of 5.0×10^{10} $M^{-1}cm^{-1}$ was compared to that from the whole blood of a mouse. The PA wave from the PNP dispersion and the blood at an excitation wavelength of 780 nm is shown in Figure 5. The PA intensities for the mouse blood and the PNP at a concentration of 10 pM were 6.45 and 10.6 kV J^{-1}, respectively. This indicates that the PA intensity from the PNP is larger than that from the blood. From the number densities for RBC of 10^7 cells/μL and the PNP dispersion of 6×10^6 particles/μL, the PA intensities from a single RBC and PNP are estimated to be 0.645 and 1.77 mV J^{-1}. Considering the volumes of a PNP-PS-160 and a RBC (0.002 and 50 fL, respectively), the PNP emits the PA signal greater than a blood. Thus, the PNP containing a NIR dye would be used as a sensitive contrast agent for *in vivo* PA imaging.

The *in vivo* photo-acoustic imaging of mice was demonstrated. Prior to the *in vivo* imaging, we confirmed that the PNP was stably dispersed in phosphate buffered saline (PBS) and fetal bovine serum (FBS) without aggregation for 2 weeks as shown in Figure S6a. Moreover, the leakage of the dye fraction into the FBS medium was not observed because of the strong hydrophobicity of SiNc (see Figure S6b). These results indicate that the PNP can be used in an *in vivo* condition. The mouse was subcutaneously injected with 20 μL of the dispersions of PNP-PS-160 and Au-NR at concentrations of 0.10 and 0.42 nM in PBS, respectively. Figure 6a indicates the fluorescence image at a wavelength range of 780 $\pm$ 10 nm under the excitation at 675 $\pm$ 15 nm. The PNP containing SiNc emits the weak fluorescence at 780 nm with a quantum efficiency of ca. 0.01. In the fluorescence image, the distribution of PNP-PS-160 is brightly

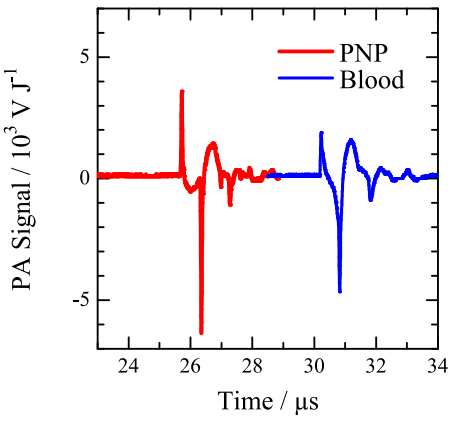

Fig. 5 Photo-acoustic wave from PNP (red) and a whole blood of a mouse (blue). The time scale for the mouse blood was shifted by 5 μs for visibility. The PNP consists of PS and SiNc, which has the diameter of 160 nm and the molar absorption coefficient of 5.0×10^{10} $M^{-1}cm^{-1}$. The mouse blood was taken from a normal nude mouse and poured into an optical cell.

observed. On the other hand, because Au-NR injected at the right hand side emits no fluorescence signal, it cannot be seen in the fluorescence image. Figure 6b shows the PA image of the 18 $\times$ 18-mm^2 area where the fluorescence of PNP-PS-160 was detected. The PA signal from the PNP was clearly detected in this image. Figure 6c shows the PA image of the Au-NR with the size of 80 $\times$ 25 nm (Au-NR-80) in a mouse. The signal intensity of the PNP was 5-times greater than that of the Au-NR-80, whereas the concentration of the PNP dispersion was 4-fold lower than that of Au-NR. The signal to noise ratios (SNR) in the PA imaging with PNP-PS-160 and Au-NR-80 were 560 and 106, respectively. The detection limit (SNR = 1) for PNP-PS-160 can be estimated to be 0.18 pM. The PNP consisting of a material with a high Grüneisen parameter would improve the signal intensity. The PNP consisting of PMMA showed the SNR of 550 at the injection concentration of 0.04 nM (shown in Figure S7). The PNP-PMMA shows the similar SNR although the concentration of the PNP of PMMA was 2.5-times lower than that of PNP-PS. This indicates the higher sensitivity of PNP of PMMA and the detection limit can be improved to several tens femtomolar. Thus, the PNP enables the *in vivo* PA imaging with higher sensitivity than the gold nano-particle probe. The blood circulation and accumulation in tissues can be optimized without changing the optical properties by the precise control of the particle size and the surface modification. For example, the PEGyrated PNP was prepared by the addition of dimyristoyl phosphatidylethanolamine-bounded polyethylene glycol (DMPE-PEG2000, NOF) in the nano-emulsion process without significant effects on the size

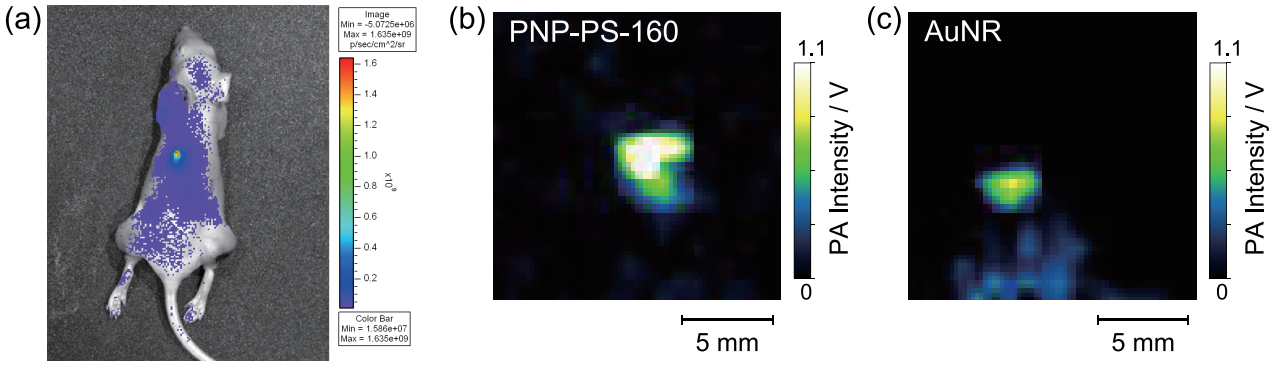

Fig. 6 *In vivo* measurements of a mouse injected with PNP and Au-NR. (a) Fluorescence image of a mouse injected with the PNP with a diameter of 160 nm, which was acquired by collecting the emission of SiNc. (b) Photo-acoustic image of the PNP observed at the fluorescent area in the panel a. (c) PA image with Au-NR-80.

distribution and PA properties (Figure S3). Thus, the PNP with a NIR dye can be used as a high sensitivity contrast agent in the *in vivo* PA imaging.

Conclusions

We showed that the polymer nano-particle (PNP) containing an NIR absorbing dye generates the strong PA signal. The enhancement of the PA signal can be achieved by the suppression of the heat transfer from the PNP to the water medium. Because of the low thermal diffusivity of polymer materials, the diffusion of the heat induced by a laser pulse from the PNP to the water medium is restricted. The thermal expansion of the PNP with the large Grüneisen parameter compared to water results in the generation of the stronger PA wave than gold nano-particles. Moreover, the spectral feature and the blood circulation of the PNP by the nano-emulsion method can be easily optimized. The polymer nano-particles with NIR dyes would be a promising contrast agent for the photo-acoustic imaging modality.

Acknowledgements

This work is supported by the Innovative Techno-Hub for Integrated Medical Bio-imaging Project of the Special Coordination Funds for Promoting Science and Technology from Ministry of Education, Culture, Sports, Science and Technology (MEXT), Japan.

Note and references

1 L. V. Wang and H.-i. Wu, *Biomedical Optics: Principles and Imaging*, Wiley-Interscience, Hoboken, 2007.
2 G. P. Luke, D. Yeager and S. Y. Emelianov, *Ann. Biomed. Eng.*, 2012, **40**, 422–437.
3 L. V. Wang and S. Hu, *Science*, 2012, **335**, 1458–1462.
4 A. de la Zerda, C. Zavaleta, S. Keren, S. Vaithilingam, S. Bodapati, Z. Liu, J. Levi, B. R. Smith, T.-J. Ma, O. Oralkan, Z. Cheng, X. Chen, H. Dai, B. T. Khuri-Yakub and S. S. Gambhir, *Nature Nanotech.*, 2008, **3**, 557–562.
5 A. de la Zerda, S. Bodapati, R. Teed, S. Y. May, S. M. Tabakman, Z. Liu, B. T. Khuri-Yakub, X. Chen, H. Dai and S. S. Gambhir, *ACS Nano*, 2012, **6**, 4694–4701.
6 D. Pan, X. Cai, C. Yalaz, A. Senpan, K. Omanakuttan, S. A. Wickline, L. V. Wang and G. M. Lanza, *ACS Nano*, 2012, **6**, 1260–1267.
7 A. Agarwal, S. W. Huang, M. O'Donnell, K. C. Day, M. Day, N. Kotov and S. Ashkenazi, *J. Appl. Phys.*, 2007, **102**, 064701–064701–4.
8 K. H. Song, C. Kim, C. M. Cobley, Y. Xia and L. V. Wang, *Nano Lett.*, 2009, **9**, 183–188.
9 X. Yang, S. E. Skrabalak, Z.-Y. Li, Y. Xia and L. V. Wang, *Nano Lett.*, 2007, **7**, 3798–3802.
10 X. Cai, W. Li, C.-H. Kim, Y. Yuan, L. V. Wang and Y. Xia, *ACS Nano*, 2011, **5**, 9658–9667.
11 Y.-S. Chen, W. Frey, S. Kim, P. Kruizinga, K. Homan and S. Emelianov, *Nano Lett.*, 2011, **11**, 348–354.
12 M. Eghtedari, A. Oraevsky, J. A. Copland, N. A. Kotov, A. Conjusteau and M. Motamedi, *Nano Lett.*, 2007, **7**, 1914–1918.
13 J. V. Jokerst, M. Thangaraj, P. J. Kempen, R. Sinclair and S. S. Gambhir, *ACS Nano*, 2012, **6**, 5920–5930.
14 G. Ku and L. V. Wang, *Opt. Lett.*, 2005, **30**, 507–509.
15 D. Razansky, C. Vinegoni and V. Ntziachristos, *Opt. Lett.*, 2007, **32**, 2891–2893.
16 S. Bhattacharyya, S. Wang, D. Reinecke, W. Kiser, R. A. Kruger and T. R. DeGrado, *Bioconjugate Chem.*, 2008, **19**, 1186–1193.
17 S. M. Moghimi, A. C. Hunter and J. C. Murray, *Pharmacol. Rev.*, 2001, **53**, 283–318.
18 W. H. De Jong and P. J. Borm, *Int. J. Nanomedicine*, 2008, **3**, 133–149.
19 S. Kim, J.-H. Kim, O. Jeon, I. C. Kwon and K. Park, *Eur. J. Pharm. Biopharm.*, 2009, **71**, 420–430.
20 N. R. B. Boase, I. Blakey and K. J. Thurecht, *Polym. Chem.*, 2012, **3**, 1384–1389.
21 T. L. Doane and C. Burda, *Chem. Soc. Rev.*, 2012, **41**, 2885–2911.
22 C. Solans, P. Izquierdo, J. Nolla, N. Azemar and M. Garcia-Celma, *Cur. Opin. Colloid Interface Sci.*, 2005, **10**, 102–110.
23 N. Anton, J.-P. Benoit and P. Saulnier, *J. Controlled Release*, 2008, **128**, 185–199.

24 E. C. Cho, C. Kim, F. Zhou, C. M. Cobley, K. H. Song, J. Chen, Z.-Y. Li, L. V. Wang and Y. Xia, *J. Phys. Chem. C*, 2009, **113**, 9023–9028.

25 S. E. Braslavsky and G. E. Heibel, *Chem. Rev.*, 1992, **92**, 1381–1410.

26 The sound pressure, P, consists of the pressure components of the volume expansion of water and PNP: $P = P_w + P_p$, where P_w and P_p are the sound pressure component by the volume expansion of the water medium and the PNP, respectively. The value of the P_p can be estimated as the sound pressure at 4°C because the expansion of water is negligible. Therefore, the pressure component at 20°C is evaluated the ratio of the PA signals at 4 and 20°C.

27 S.-S. Chang, C.-W. Shih, C.-D. Chen, W.-C. Lai and C. R. C. Wang, *Langmuir*, 1999, **15**, 701–709.

28 J. Brandrup, E. H. Immergut, E. A. Grulke, A. Abe and D. R. Bloch, *Polymer Handbook*, John Wiley & Sons, New York, 4th edn, 1999.

29 E. Morita, R. Kono and H. Yoshizaki, *Jpn J. App. Phys.*, 1968, **7**, 451–461.

30 A. M. North, R. A. Pethrick and D. W. Phillips, *Polymer*, 1977, **18**, 324–326.

31 I. G. Calasso, W. Craig and G. J. Diebold, *Phys. Rev. Lett.*, 2001, **86**, 3550–3553.

32 G. J. Diebold, A. C. Beveridge and T. J. Hamilton, *J. Acoust. Soc. Am.*, 2002, **112**, 1780–1786.